IOP PUBLISHING JOURNAL OF PHYSICS D: APPLIED PHYSICS

J. Phys. D: Appl. Phys. **42** (2009) 145115 (6pp) doi:10.1088/0022-3727/42/14/145115

The role of bulk and interface states on performance of a-Si : H p-i-n solar cells using reverse current–voltage technique

S A Mahmood[1], R V R Murthy[2], M Z Kabir[1] and V Dutta[3]

[1] Department of Electrical and Computer Engineering, Concordia University, 1455 Blvd. de Masionneuve West, Montreal, Quebec, H3G 1M8, Canada
[2] PerkinElmer Optoelectronics, 22001 Dumberry Road, Vaudreuil, Quebec, J7V 8P7, Canada
[3] Photovoltaic Laboratory, Center for Energy Studies, Indian Institute of Technology, New Delhi 110 016, India

E-mail: murthy.rambhatla@perkinelmer.com

Received 15 January 2009, in final form 5 May 2009
Published 1 July 2009
Online at stacks.iop.org/JPhysD/42/145115

Abstract

The defect state densities in the bulk of the i-layer and at the p/i interface have been studied in hydrogenated amorphous silicon (a-Si : H) solar cells using reverse current–voltage (J–V) measurements. In this work the cells have been soaked with blue and red lights prior to measurements. The voltage-dependent reverse current has been analysed on the basis of thermal generation of the carriers from midgap states in the i-layer and the carrier injection through the p/i interface. Based on the reverse current behaviour, it has been analysed that at lower reverse bias (reverse voltage, $V_r < 5$ V) the defect states in the bulk of the i-layer and at higher bias ($V_r \sim 25$ V) the defect states at the p/i interface are contributing to the reverse currents. The applied reverse bias annealing (RBA) treatment on these cells shows more significant annihilation of defect states at the p/i interface as compared with the bulk of the i-layer. An analytical model is developed to explain the observed behaviour. There is good agreement between the theory and the experimental observations. The fitted defect state densities are 9.1×10^{15} cm^{-3} and 8×10^{18} cm^{-3} in the bulk of the i-layer and near the p/i interface, respectively. These values decrease to 2.5×10^{15} cm^{-3} and 6×10^{17} cm^{-3}, respectively, in the samples annealed under reverse bias at 2 V.

1. Introduction

Amorphous silcon (a-Si : H) thin film solar cells and modules have been receiving a great deal of attention as a low cost source of electrical generation. Achieving high efficiency is a key requirement in these cells to bring down the cost. The cell efficiency and performance are mainly being controlled by the quality of the p/i interface and the intrinsic i-layer in terms of defect state densities in the primitive single junction p-i-n structure. Several characterization techniques have been performed and their results are analysed systematically in the past, in order to understand the role of these defect states on the overall performance of the cell [1–4]. Among these, current–voltage (J–V) is one of the powerful techniques for determining the defect states within the mobility gap of a-Si : H.

The dark reverse current in a-Si : H p-i-n solar cells has been identified to stem from various sources such as contact injection, shunt leakage and thermal generation [5]. In well-passivated devices with high quality of p and n contacts, the contact injection mechanism is neglected. The shunt current is probably caused by inhomogeneities in and short circuits between the solar cell layers during the deposition process. One can easily find out this effect from reverse J–V characteristics in a small voltage range as long as the device behaves ohmic. The thermal generation is traditionally described by Shockley–Read–Hall (SRH) statistics in which the generation rate is determined by the thermal emission of

Table 1. (*a*) The deposition parameters of the cells used in these measurements and (*b*) the typical properties of individual layers used in a-Si : H solar cells.

(a) The deposition parameters of the cells used in these measurements

Deposition technique	Plasma CVD (multiple chamber)
Substrate temperature (°C)	180
Gas flow rate (SCCM)	100
Power (W cm^{-2})	0.1
Pressure (mTorr)	500

(b) The typical properties of individual layers used in a-Si : H solar cells

Layers	Doping ratio	Dark and photo conductivities (Ω^{-1} cm^{-1})	E_g (eV)
p$^+$-layer	$SiH_4 : CH_4 : B_2H_6 \sim 1 : 1 : 0.006$	5×10^{-5}, —	1.94
i-layer	SiH_4 (undoped)	10^{-10}, 5×10^{-5}–10^{-4}	1.77
n$^+$-layer	$SiH_4 : PH_3 \sim 1 : 0.004$	10^{-2}, —	1.80

holes or electrons from deep states. The study of reverse currents as a function of voltage, which is controlled by thermal generation, can yield useful information about the midgap states and their spatial distribution in the i-layer. Several groups have studied voltage-dependent reverse current behaviour in these devices [6–14]. Street has analysed reverse current behaviour by Poole–Frenkel enhanced generation [11, 12] based on the assumption of a uniform distribution of defect states over the i-layer within a narrow energy region. Arch *et al* have analysed the current behaviour based on spatially varying defects in the bandgap [13, 14]. However, an understanding of the possible underlying mechanism and the explicit model is somewhat limited, if not inconsistent. Moreover, the reverse J–V study under different light induced degradation differentiates the bulk and interface impacts and reveals the type of defects. The use of blue and red photons can be very effective, since these photons will be absorbed within 10–20 nm and 100–200 nm in the i-region, respectively, from the p/i interface. If blue photons are incident from the p-side, apart from information regarding the electron traps in the i-layer, the information on the interface states at the p/i junction can be obtained. If red photons are incident from the p-side, apart from information regarding the electron and hole traps in the i-layer, the information on the bulk states can be obtained.

Reverse bias annealing (RBA) improves the a-Si : H p-i-n solar cell performance. This concept has already been discussed by Swartz [15], Fortmann [16] and Carlson *et al* [17], but the reasons for this improvement are different from one another. Swartz has shown that this improvement is due to the increase in the acceptor concentration in the p-layer. Fortmann has investigated that this improvement is due to the improvement in the i-layer. Carlson has shown that the suppression of degradation is due to the reduction in hydrogen diffusion under reverse bias at temperatures less than 180 °C. In another report, Kleider has shown that RBA leads defect creation in the a-Si : H schottky diodes [18]. Therefore, in order to understand this behaviour, a detailed study of the thermal annealing in these devices is necessary.

In this paper, we perform reverse current–voltage studies on as-deposited and reverse bias annealed samples in p-i-n a-Si : H solar cells after degrading the cells with blue and red lights in order to determine the defect states and the effects of annealing on the defect states in the bulk of the i-layer and at the p/i interface. We have developed an analytical expression for the steady-state thermal generation current by solving the continuity equation for both electrons and holes. The voltage-dependent total dark current is obtained by adding thermal generation current with the steady-state injection current through the p/i interface. The dark current model is compared with the measured experimental data. The fitting of the model with the experimental data estimates the concentration of defect states in the i-layer and near the p/i interface.

2. Experimental details

Current–voltage (J–V) measurements have been carried out on a-Si : H solar cells of structure of glass/ITO/p$^+$(15 nm)/i(350 nm)/n$^+$(20 nm)—a-Si : H/Ag. The deposition parameters and properties of each layer have been shown in tables 1(*a*) and (*b*). The i-layers of the samples used in our measurements are slightly n-type with Fermi energy level (E_F) at 0.65 eV below the conduction band edge (E_C). Small samples of area 1 cm^2 have been used in our measurements. The blue ($\lambda = 450$ nm) and red ($\lambda = 670$ nm) lights with an intensity of 100 mW cm^{-2}, which were obtained from a white light with a combination of cut-off (650 nm) and cut-on (500 nm) optical filters, had been used for degrading the cells. The required light intensity was achieved by passing the light through a set of convex lenses. The reverse biased annealing (RBA) treatment was performed on two sets of samples, one set degraded with blue light and the other set with red light, under different reverse biases (reverse voltage, $V_r = 0$ V, 1 V and 2 V) in a vacuum chamber of 10^{-6} Torr at 170 °C for 2 h. Similarly, a third set of samples (as-deposited) were also degraded with blue and red lights at room temperature for 2 h prior to measurements. The as-deposited sample is referred to as sample A. The samples annealed at 0 V, 1 V and 2 V reverse biases are referred to as samples B, C and D, respectively.

3. Analytical model

In p-i-n a-Si : H solar cell structures with doped layers that provide good blocking contacts (at metal/semiconductor interface), the principal sources of the steady-state dark current are the thermal generation through the defect states in the i-layer and the emission of carriers from the p/i and i/n interfaces [13]. The i-layer is slightly n-type and thus the Fermi level E_F at zero bias is above the midgap. After applying the bias, electrons are depleted from the i-layer and the quasi-Fermi level E_{FD} lies below E_F. Assuming uniform carrier depletion throughout the i-layer, the steady-state electric fields at the p/i interface and n/i interfaces can be written as

$$F_1 = F_0 + \frac{eLn_d}{2\varepsilon_s} \tag{1}$$

and

$$F_2 = F_0 - \frac{eLn_d}{2\varepsilon_s}, \tag{2}$$

where $F_0 (= V/L)$ is the applied field, V is the bias voltage, L is the intrinsic layer thickness, $\varepsilon_s (= \varepsilon_0\varepsilon_r)$ is the permittivity of the amorphous silicon, e is the elementary charge and F_1 and F_2 are the electric fields at the p/i and n/i interfaces, respectively. Here n_d is the steady-state depleted electron concentration in the i-layer, which can be written as

$$n_d = \int_0^{E_c} N(E)\left\{\frac{1}{1+\exp[(E-E_F)/kT]} - \frac{1}{1+\exp[(E-E_{FD})/kT]}\right\} dE, \tag{3}$$

where $N(E)$ is the density of states of a-Si : H at energy E in the midgap, k is the Boltzmann constant and T is the absolute temperature.

The steady-state thermal generation current in a-Si : H detectors arises from the carriers excited from the deep states near E_{FD} to the band edges in the intrinsic layer. The perturbation of applied electric field in the i-layer due to the space charge is usually very small. As the electric field near the p/i interface is slightly higher than that near the n/i interface, the thermally generated carriers will move with a slightly higher velocity near the p/i interface compared with that near the n/i interface. Therefore, assuming a constant average drift velocity of the carriers throughout the sample will not make any significant difference in the calculation of charge collection. Under thermal equilibrium condition, the trap levels are identified with the neutral defect observed by electron-spin resonance [19]. Therefore, the trapped electron and hole states are most likely charged defect (positive or negative) states and thus field enhanced thermal generation is neglected. Considering uniform thermal emission of trapped carriers throughout the i-layer, the continuity equation of electrons at reverse bias can be written as

$$\frac{\partial n(x,t)}{\partial t} + \mu_e F_0 \frac{\partial n(x,t)}{\partial x} = -\frac{1}{\tau_e} n(x,t) + g, \tag{4}$$

where μ_e is the drift mobility of electrons, τ_e is the effective electron lifetime, t is the time, x is the distance from the p/i interface and n is the concentration of electrons. For a-Si : H, the thermal generation rate is dominated by the carrier generation from traps within kT of E_{FD}. If the excitation rates for electrons and holes are equal, E_{FD} is very close to the middle of bandgap. The generation rate for a fully depleted sample is determined by the average carrier release time and is given by [5]

$$g = N(E_{FD})kT\omega_0 \exp[-(E_C - E_{FD})/kT], \tag{5}$$

where ω_0 is the attempt-to-escape frequency. It is assumed in equation (5) that the density of states is constant over kT near E_{FD}. At steady state, the solution of (4) is

$$n(x) = g\tau_e\left[1 - \exp\left(-\frac{x}{\mu_e\tau_e F_0}\right)\right]. \tag{6}$$

The electron current density is given by

$$J_e = \frac{e\mu_e F_0}{L}\int_0^L n(x)\,dx. \tag{7}$$

Therefore, the steady-state thermal generation current is

$$J_{e(h)} = e\mu_{e(h)}\tau_{e(h)}F_0 g\left[1 - \frac{\mu_{e(h)}\tau_{e(h)}F_0}{L} \times \left\{1 - \exp\left(-\frac{L}{\mu_{e(h)}\tau_{e(h)}F_0}\right)\right\}\right]. \tag{8}$$

Subscripts e and h stand for electrons and holes, respectively. It is evident from equation (8) that the current depends on the applied field due to trapping of the generated carriers.

In the p-i-n structure, besides thermal generation in the i-layer, electron injection through the p/i interface is a possible source of current at higher fields. Hole injection through the n/i interface is negligible because of the lower electric field at the n/i interface [20] (this is also evident from equations (1) and (2)) and its low mobility. The p/i interface is a high field region, contains a high defect density and thus, at room temperature, interface field enhanced generation can be the dominating process at higher applied fields [21]. The carriers are injected from the distributed trap states near E_{FD} at the p/i interface. We can define an effective barrier height ϕ_{eff} for the injected electrons. The width of the depletion layer in the p-region, w_p, depends on the doping concentration of the p-layer, and the carrier generation rate near the p/i interface depends on the effective trap density at the interface [21]. Assuming full depletion of the i-layer and a constant quasi-Fermi level in the p-layer, the reverse current density due to the carrier generation within w_p and subsequent electron injection through the p/i interface can be written as [10, 22]

$$J_{inj} = ew_p g_p \cong \left(\frac{\varepsilon_s F_1}{N_a}\right) N_t\omega_0 \exp\left\{-\frac{\phi_{eff} - \beta_{pf}\sqrt{F_1}}{kT}\right\}, \tag{9}$$

where g_p is the carrier generation rate at the p/i interface, N_a is the active dopant concentration in the p-layer, N_t is the effective trap density at the p/i interface and $\beta_{pf} = \sqrt{e^3/\pi\varepsilon}$ is the Poole–Frenkel coefficient. Therefore, the total steady-state dark current in a-Si : H p-i-n solar cell is $J = J_e + J_h + J_{inj}$.

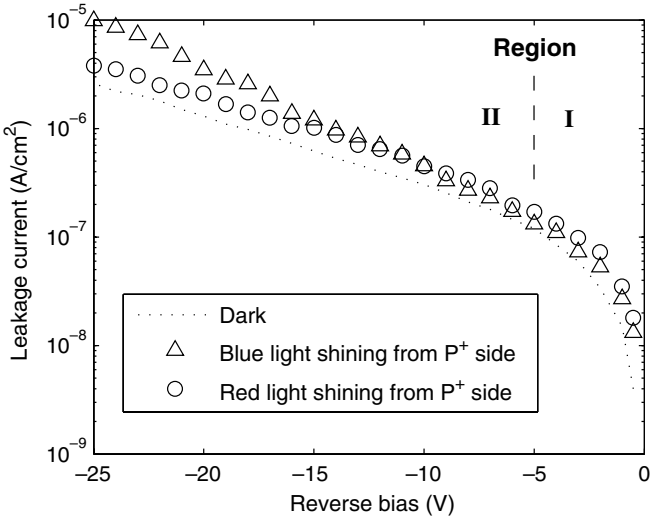

Figure 1. Reverse current as a function of voltage in a-Si : H solar cell.

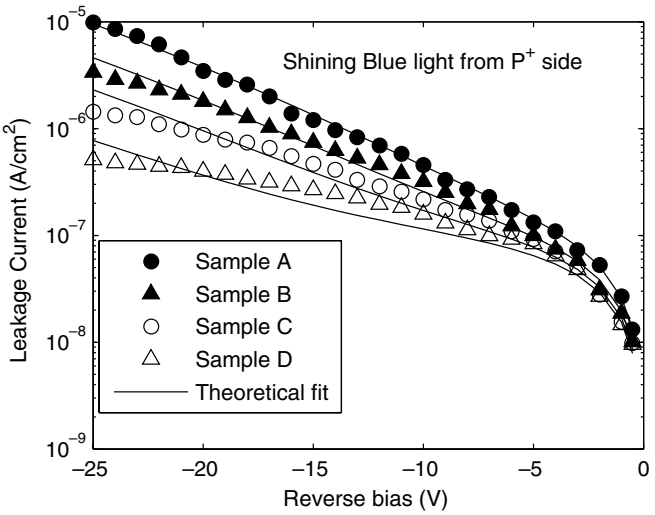

Figure 2. Reverse current as a function of voltage for as-deposited (sample A) and reverse bias annealed (samples B, C and D) samples of a-Si : H solar cells after degrading with blue light for 2 h. The symbols represent experimental data and the solid lines represent the theoretical fit to the experimental data.

4. Results and discussion

The J–V characteristics of as-deposited sample A, after soaking the cells by shining blue and red lights through the p-side, are shown in figure 1. The voltage-dependent current behaviour can be divided into two regions. The current rises steeply in region I ($V_r \leqslant 5$ V) and increases exponentially in region II ($V_r > 5$ V) as a function of voltage. The reverse current in region I is slightly higher in the red light soaked sample as compared with the blue light soaked sample. However, this difference is significant in region II where the reverse current is higher in the blue light soaked sample as compared with the red light soaked sample. The J–V characteristic in the dark is also shown therein as a reference. As mentioned earlier, the photons from the blue light are absorbed within 10–20 nm in the i-region near the p/i interface. Thus, the observed high reverse current in region II in the blue light soaked sample is due to the degradation of the p/i interface zone. On the other hand, the high reverse current in region I in the red light soaked sample is due to the degradation of the bulk of the i-layer. Generally, the high dark current in the high voltage region in the standard p-i-n structures was explained in the literature either by contact injection due to the defective p/i interface [5] or by boron diffusion from the p-layer to the i-layer at the interface [9]. The p- and n-layers in our cells are thick enough to control the contact injection. Moreover, we have not observed any change in reverse current with time after voltage application in our samples during the data collection. Secondly, the p type graded a-SiC : H layer in our samples act as an effective blocking layer to minimize the boron diffusion. Here, we still assume that the electron injection at the p/i interface presumably contribute to this current, which is not a function of time.

The impact of RBA on the samples that are soaked with blue and red lights are shown in figures 2 and 3, respectively. The reverse current for sample A (as-deposited) is higher than that for the annealed samples in the entire voltage region due to interface and bulk degradations. In the blue light

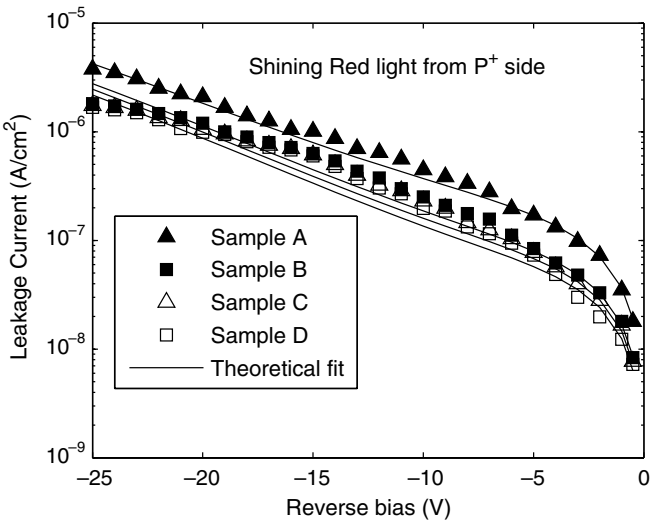

Figure 3. Reverse current as a function of voltage for as-deposited (sample A) and reverse bias annealed (samples B, C and D) samples of a-Si : H solar cells after degrading with red light for 2 h. The symbols represent experimental data and the solid lines represent the theoretical fit to the experimental data.

shined samples (figure 2), the reverse current depends on the annealing treatment and degradation. The reduction in the reverse current in region II is more prominent in samples C and D. This indicates that the RBA treatment improves the p/i interface properties. Based on the facts mentioned earlier, a more likely explanation for observed improvement by the RBA treatment is due to the diffusion of hydrogen towards the p/i interface in the presence of electric field and temperature [23] because of rich hydrogen content in the i-layer near the interfaces [24]. There may be two types of effects at the interface. Firstly, this hydrogen may link with silicon dangling bonds and reduce the defect states. Secondly, the hydrogen may interact with impurities such as oxygen and

Table 2. The fitted values of density of states and carrier lifetimes.

Incident photons	Samples	$N(E_{FD})$ ($cm^{-3}\,eV^{-1}$)	τ_e (s)	τ_h (s)	N_t (cm^{-3})
Blue	A	2.3×10^{17}	1×10^{-10}	1×10^{-10}	8×10^{18}
	B	1.7×10^{17}	1.1×10^{-10}	1.1×10^{-10}	4×10^{18}
	C	1.4×10^{17}	1.2×10^{-10}	1.2×10^{-10}	2×10^{18}
	D	1.2×10^{17}	1.3×10^{-10}	1.3×10^{-10}	6×10^{17}
Red	A	3.5×10^{17}	1×10^{-10}	1×10^{-10}	3×10^{18}
	B	1.5×10^{17}	1.1×10^{-10}	1.1×10^{-10}	2.4×10^{18}
	C	1.2×10^{17}	1.2×10^{-10}	1.2×10^{-10}	2.2×10^{18}
	D	9.5×10^{16}	1.3×10^{-10}	1.3×10^{-10}	2×10^{18}

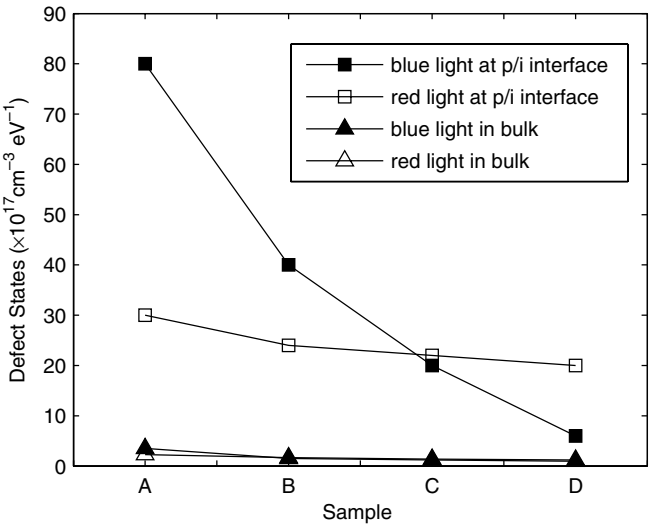

Figure 4. Defect density variation with RBA treatment.

then remove them by creating volatile species [25]. Eventually, these mechanisms presumably reduce the electron injection significantly at the p/i interface.

In the red light soaked samples (figure 3), the difference in the reverse currents for samples B, C and D is quite negligible. However, there is a significant difference between the reverse current in sample A and the other annealed samples. This difference in reverse current suggests that there is indeed a decrease in bulk defect state density in the i-layer due to thermal annealing.

The results of our steady-state dark current model are shown in figures 2 and 3 along with the experimental results for the blue and red light soaked samples. The values of the parameters that are used in the calculation are $\mu_e = 0.5\,cm^2\,V^{-1}\,s^{-1}$, $\mu_h = 0.003\,cm^2\,V^{-1}\,s^{-1}$, $\omega_0 = 10^{13}\,s^{-1}$, $\phi_{eff} = 1.0\,eV$, $E_C - E_F = 0.65\,eV$, $E_C - E_{FD} = 0.7\,eV$ and $N_a \approx 1 \times 10^{17}\,cm^{-3}$ [5, 26, 27]. The best values of the fitting parameters are given in table 2. The modelling results show a fair match with the experimental observations. The defect state density variation, both at the p/i interface and in the bulk, with the RBA treatment has been shown in figure 4. As expected, the modelling shows that the RBA treatment decreases the defect states at the p/i interface significantly as compared with the bulk of the i-layer.

5. Conclusions

The roles of bulk and interface in a-Si : H p-i-n solar cells using reverse current–voltage characteristics are identified. The current due to thermal generation in different voltage regions is analysed. It has been observed that the reverse current in the low voltage region is due to defect states in the i-layer whereas the reverse current in the higher voltage region is due to interface states at the p/i junction. The effect of the RBA treatment on these cells was observed more near the p/i interface as compared with the bulk of the i-layer. The expression for the bias-dependent steady-state reverse current behaviour has been developed and fitted with the experimental results. The defect state densities have been estimated to be $9.1 \times 10^{15}\,cm^{-3}$ and $8 \times 10^{18}\,cm^{-3}$, respectively, in the bulk of i-layer and at the p/i interface. These defect densities reduce to $2.5 \times 10^{15}\,cm^{-3}$ and $6 \times 10^{17}\,cm^{-3}$ by the RBA treatment, respectively.

Acknowledgments

The authors would like to thank the University Grants Commission, New Delhi, and the NSERC for financial assistance.

References

[1] Madan A, Le Comber P G and Spear W E 1976 *J. Non-Cryst. Solids* **20** 239
[2] Lang D V, Cohen J D and Harbison J P 1982 *Phys. Rev.* B **25** 5285
[3] Kalina J, Schade H and Delahoy A E 1989 *Sol. Cells* **27** 341
[4] Deng J, Rross B, Albert M, Collins R and Wronski C 2006 *Mater. Res. Soc. Symp. Proc.* **910** 0910-A02-02
[5] Street R A 1991 *Phil. Mag.* B **63** 1343
[6] Johnson T R, Ganguly G, Wood G S and Carlson D E 2003 *Mater. Res. Soc. Symp. Proc.* **762** A7.7.1
[7] Tchkarov S, Roca i Cabarrocas, Dutta U, Chatterjee P and Equer B 2003 *J. Appl. Phys.* **94** 7317
[8] Morrison S, Servati P, Vygraneko Y, Nathan A and Madan A 2002 *Mater. Res. Soc. Symp. Proc.* **715** A7.4.1
[9] Theil J A 2003 *Mater. Res. Soc. Symp. Proc.* **762** A21.4.1
[10] Kim H J, Cho G, Choi J and Jung K-W 2002 *Appl. Phys. Lett.* **80** 4843
[11] Street R A 1990 *Appl. Phys. Lett.* **57** 1334
[12] Street R A 1991 *Appl. Phys. Lett.* **59** 1084
[13] Arch J K and Fonash S J 1992 *Appl. Phys. Lett.* **60** 757

[14] Arch J K and Fonash S J 1992 *J. Appl. Phys.* **72** 4483
[15] Swartz G A 1984 *Appl. Phys. Lett.* **44** 697
[16] Fortmann C M 1988 *Proc. 8th EC Photovoltaic Science and Engineering Conf. (Florence, Italy)* (Dordecht: Kluwer) p 929
[17] Carlson D E and Rajan K 1996 *Appl. Phys. Lett.* **68** 28
[18] Kleider J P and Roca i Cabarrocas P 2002 *J. Non-Cryst. Solids* **299–302** 599–604
[19] Street R A 1991 *Hydrogenated Amorphous Silicon* (*Cambridge Solid State Science Series*) (Cambridge: Cambridge University Press) p 104
[20] Cerdeira A and Estrada M 2000 *IEEE Trans. Electron. Dev.* **47** 2238
[21] Chévrier J B and Equer B 1994 *J. Appl. Phys.* **76** 7415
[22] Mahmood S A, Kabir M Z, Tousignant O, Mani H, Greenspan J and Botka P 2008 *Appl. Phys. Lett.* **92** 223506
[23] Rothwarf A 1988 *Proc. 20th IEEE Photovoltaic Specialists Conf. (Las Vegas, NV)* (New York: IEEE) p 166
[24] Neitzert H C, Briere M A and Lechner P 1991 *Physica* B **170** 529
[25] Imao S, Nakajima S, Nakata J I, Hattori R, Shirafuji J and Inuishi Y 1991 *Japan. J. Appl. Phys. Lett.* **30** L1227
[26] Street R A (ed) 2000 *Technology and Applications of Amorphous Silicon* (Berlin: Springer) p 151
[27] Wieczorek H 1995 *Solid State Phenom.* **44–46** 957